Available online at www.sciencedirect.com

ScienceDirect

Biochimie Open 2 (2016) 1–8

http://www.journals.elsevier.com/biochimie-open

Research paper

Uncovering the role of the flexible C-terminal tail: A model study with Strep-tagged GFP

Michael W. Lassalle [a,*], Shinobu Kondou [b]

[a] *iCLA (International College of Liberal Arts), Yamanashi Gakuin University, 2-4-5 Sakaori, Kofu-city, Yamanashi-ken, 400-8575 Japan*
[b] *Ehime Prefectural Police HQ, Forensic Science Laboratory, Japan*

Received 12 October 2015; accepted 18 November 2015
Available online 30 November 2015

Abstract

Recently, it has been recognized that, much like an electric current in an electric circuit, dynamic disruptions from flexible, unstructured regions distal to the active region are transferred through the contact network to the active site and influence protein stability and/or function. As transmembrane proteins frequently possess the β-barrel structure, studies of proteins with this topology are required. The unstructured lid segments of the β-barrel GFP protein are conserved and could play a role in the backbone stabilization required for chromophore function. A study of the disordered C-terminus and the function within the lid is necessary. In this study, we entirely truncated the flexible C-terminal tail and investigated the N-terminal Strep-tagged GFP by fluorescence spectroscopy, and the temperature- and GdnHCl-induced unfolding by circular dichroism. The introduction of the unstructured Strep-tag itself changed the unfolding pathway. Truncating the entire flexible tail did not decrease the fluorescence intensity to a large extent; however, the protein stability changed dramatically. The temperature for half-denaturation $T_{1/2}$ changed significantly from 79 °C for the wild-type to 72.8 °C for the mutant. Unfolding kinetics at different temperatures have been induced by 4 M GdnHCl, and the apparent Arrhenius activation energy decreased by 40% as compared to the wild-type.

Keywords: Intrinsically unfolded protein tails (IDPTs); Activation energy; GdnHCl-induced unfolding; Protein flexibility and function

1. Introduction

Research on dihydrofolate reductase revealed that single amino-acid substitutions in flexible loops play important roles in determining the enzyme function [1]. Mutations in unstructured regions have severe outcomes for our health, as shown for familial hypertrophic cardiomyopathy (FHC) and hypertrophic cardiomyopathy (HCM), diseases closely related to sudden death [2]. Human cardiac troponin is an allosteric-coupled protein with intrinsically unfolded regions, and around 80% of all FHC-causing mutations in human cardiac troponin are in regions with no, or only nascent, structure [3]. For the G203 mutation in human cardiac troponin, a troponin paradox existed. Experimental observations led to the conclusion that any mutation within residues 199–210 should have no effect on either inhibition or ATPase activity, but the G203S mutation affected the inhibitory affinity of cardiac troponin I [4]. Carefully performed NMR relaxation measurements resolved this paradox [3]. The correlation time decreased not only near the mutation side, but also throughout the whole unfolded C-terminal tail. Those global dynamic changes are responsible for the disease-causing effect of G203S. A novel tool for protein engineering appeared. As for varicella zoster virus thymidine kinase activity [5], drug function could be regulated by mutations distal to the substrate site. Intrinsically disordered proteins appeared as a potential drug target [6]. Similar results have been obtained for *Escherichia coli* dihydrofolate reductase [7]. Contact networks have been revealed that related well to the observed long-range chemical shift perturbations (global dynamic

* Corresponding author. Tel.: +81 55 224 1988.
E-mail address: mwlassalle@ygu.ac.jp (M.W. Lassalle).

http://dx.doi.org/10.1016/j.biopen.2015.11.004

changes). Obviously, unstructured, flexible regions exhibit a significant effect on protein function, stability and dynamics. β-barrel membrane proteins have diverse functions such as ion transportation, nutrient intake and defense against attack proteins [8]. As transmembrane proteins require a lipid bilayer to retain their structural integrity, GFP is a model protein widely used to understand the function of β-barrel proteins. It has been recognized that the unstructured, flexible C-terminal tail might be important for the fluorescence activity [9,10]. Systematic deletion studies have been performed qualitatively by FACS (fluorescence-activated cell sorting) analysis [9,10]. To further understand the role of this region for protein function and stability of GFP, we performed a more rigorous quantitative analysis by fluorescence and circular dichroism spectroscopy.

2. Material and methods

2.1. Cloning, overexpression and purification

The p53 DNA was cloned into the KpnI, Hind III cloning site of the pET-51b(+) plasmid. It was provided by the CSTRC Center of Ehime University. This GFP protein contains three mutations. The Q80R mutation is caused by PCR errors in the original cloning of GFP. In some GFP genes this error has been corrected, while in other wild-types of GFP it has not. The GTG codon at the beginning (V) enhances translational initiation and is also used in EGFP [11]. The S65T mutation increases brightness [12].

Overexpression was induced in Bl21(DE3) cells by adding 1 mM IPTG at OD = 0.5−0.6 and growing overnight at 25 °C. For this study, five mutations have been constructed − c-226, c-227, c-229, c-232 and c-235 − as shown in Fig. 1.

For purification of the proteins, and in accordance with the standard protocols, a combination of an anion exchange open column, a Strep-tag column and a high-resolution anion exchange column was used.

2.2. CD, UV and fluorescence measurements

As a buffer, 10 mM Na_2HPO_4, 10 mM KH_2PO_4, 1 mM EDTA, and 15 mM NaCl, at pH 7.6, was utilized. Protein concentration was determined by UV spectroscopy, and the absorption coefficient for each mutant was calculated by the program "Program Calculator v.3.3" (a newer version has recently become available; protcalc.sourceforge.net).

Unfolding was induced by a jump to 4 M GdnHCl at a protein concentration of 0.3 mg/ml and observed at 217 nm with a J-820 (Jasco, Japan) with a 0.1 cm cuvette. Mixing of the protein, saturated GdnHCl solution and buffer was done manually. The parameters were as follows: sensitivity standard, 217 nm wavelength, 0.5 s step resolution, and 1 nm bandwidth. Temperature-induced unfolding curves with a heating rate of 1 °C/min were measured. The following parameters were used: sensitivity standard, 217 nm, 0.2 °C step resolution, 2 s response time, 1 nm bandwidth.

The time course of ellipticity was analyzed as an apparent first-order unfolding process:

$$\theta = \theta_\infty + (\theta_0 - \theta_\infty) \times e^{-k_{obs}t} \quad (1)$$

Θ_0 is the ellipticity at 217 nm of the native protein, andΘ_∞ is the ellipticity after unfolding.

Strep-tagged GFP unfolds in a complex pathway best described by the following reaction schemes: N ↔ D; D + D → A_2 and D + D_j → A_n(j = 2,3,4), considering association-limited kinetics. In association-limited kinetics the association of the monomers [D] and aggregates is significantly slower than the preceeding steps, folding-unfolding is therefore in a pseudo equilibrium.

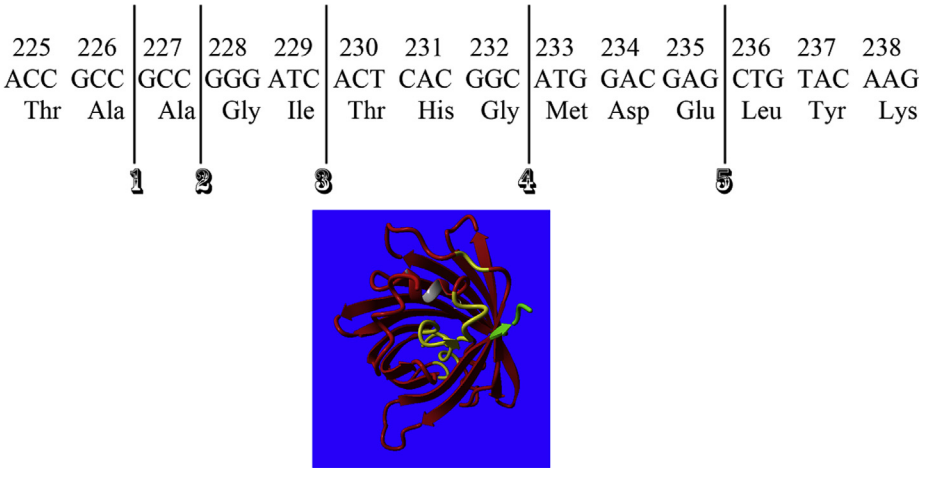

Fig. 1. Analysis of C-terminal deletion mutants of Strep-tagged GFP. The C-terminal deletions of GFP schematic represented in this figure were made by PCR/cloning, transferred into BL21(DE3), overproduced, purified and analyzed. (1: c-226; 2: c-227; 3: c-229, 4: c-232; 5: c-235). The molecular structure of GFP (PDB: 1GFL), with the C-terminal amino acids 227 to 230 colored in green, is shown. The backbone required for chromophore synthesis and the highly conserved residues near the C-terminus are colored yellow. The C-terminal residues 231 to 238 are not resolved by x-ray crystallography.

$$[N] = \frac{1}{1+K}[M] = \left(1 - f_{D,eq}\right)[M]$$
$$[D] = \frac{K}{1+K}[M] = f_{D,eq}[M] \quad (2)$$

In these equations $f_{D,eq}$ is the equlibrium fraction of the denatured monomer, defined as $\frac{K}{1+K}$, and the total monomer concentration of GFP is expressed as [M] = [N] + [D] for the pseudoequilibrium of the N ↔ D transition. As the amount of D_j is not detectable, the full set of rate coefficients can not be obtained. Roberts et al. [13] derived equations by taking the monomer concentration [M], as a function of time, into account. Assuming that all association steps are irreversible, following expression can be derived:

$$\frac{d[M]}{dt} = -2k_{D,D}f_{D,eq}^2[M]^2 - \left(\sum_{j=2}^{n^*-1} k_{1,j}[A_j]\right) f_{D,eq}[M] \quad (3)$$

with $k_{D,D}$: $D + D \xrightarrow{k_{D,D}} A_2$, $k_{i,j}$: $D + D_j \xrightarrow{k_{1,j}} A_n$ $(j = 2, 3, 4)$

Furthermore, it was shown that the summation over all aggregate states achieves a pseudo steady-state condition. Under this conditions a numerical solution can been derived:

$$\frac{d[M]}{dt} = -\sqrt{k_{D,D}\left(k_{1,j}\right)}\left(f_{D,eq}\right)^{3/2}C_o[M] = -k_{obs}C_o[M] \quad (4)$$

with C_o the monomer concentration of GFP.

If C_0, the initial concentration, is kept constant, a first-order behavior is expected and k_{obs} will be determined by Equation (1). A more detailed derivation and description of aggregation kinetics can be found in the book edited by Regina M. Murphy [13].

For temperature-induced unfolding curves, linear least square lines are calculated for the unfolded and native state and extrapolated to both ends of the melting curve to calculate the degree of unfolding.

$$\alpha = \frac{y - y_N}{y_D - y_N} \quad (5)$$

Temperature-induced unfolding has been evaluated with the van't Hoff equation to an apparent two-state model:

$$\ln K = \ln\frac{\alpha}{1-\alpha} = -\frac{\Delta H_{vH}}{RT} + \text{const} \quad (6)$$

The van't Hoff equation is valid for a two-state transition, but the temperature-induced unfolding of GFP is irreversible; therefore, the ΔH_{vH} is an apparent value that should be used only as an indicator for significant changes. The temperature for half-denaturation $T_{1/2}$ (degree of unfolding $\alpha = 0.5$) is the most valuable information for the irreversible unfolding of GFP.

Furthermore, to visualize the dramatic changes, initial temperature-jump measurements were performed by a temperature jump from 25 °C to 74 °C.

The activation energy was calculated following the Arrhenius equation

$$\ln k_{obs} = \ln A - \frac{E_A}{RT} \quad (7)$$

Emission and absorption spectra of fluorescence were measured with a Hitachi F-2500 to compare quantitatively the fluorescence activity of the wild-type and mutants.

3. Results

3.1. Fluorescence intensity

Initially, all proteins were expressed in 50 ml LB (Luria Broth) culture. Visual inspection of the expressed protein in BL21(DE3) cells showed that for the wild-type, the c-235 protein, and for the shorter mutants, including c-229, a significant decrease in fluorescence was not observed (Fig. 2). In contrast, a lower fluorescence intensity of the c-227 mutant and the c-226 GFP protein was detectable (Fig. 2). These results are similar to the previous publication [9].

For the c-226 protein, we failed to purify the protein with 50 ml LB. We had to increase the culture medium to at least 1l; this was a 20-fold increase, and yet the final protein concentration was comparable to the wild-type expressed in 50 ml LB media. Consequently, we repeated the visual inspection with purified GFP adjusted to the identical protein concentration (Fig. 3). In this publication, we will focus on the c-226 mutation that showed the largest changes. Under identical protein concentration, no difference in fluorescence is observable.

Finally, to quantify our results, we measured the emission and excitation spectra of the wild-type and the mutant at 0.05 mg/ml (Fig. 4). The excitation (max) at 491 nm is the same for the wild-type and mutant, which is reasonably close to that of GFP-S65T (489 nm). The emission (max) at 511 nm is identical for both the wild-type and mutant and close to that of GFP-S65T (509 nm). Only a 10% decrease in emission intensity (117.45 wild-type; 105.43 mutant) and an 18% decrease for the excitation intensity (118.36 wild-type; 100.08 mutant) were observed.

If comparison is related to the cell amount, a dramatic decrease in fluorescence is observable, but under identical protein concentration, the change in fluorescence is quite small and not detectable by visible inspection. One might argue that the Strep-tag plays a crucial role. For His_6-GFP, it was reported that a 13 amino-acid deletion diminished the fluorescence intensity [14]. But this study was performed with the same systematic error as the previous publication; the cell amount, and not the protein concentration, had been controlled.

3.2. Unfolding studies

Temperature-induced unfolding studies were performed, and a significant decrease in the mean residue ellipticity value was observed (Fig. 5A; green unfolding curve).

It is known that β-sheet proteins, such as CD-2, with α-helical propensities can unfold to intermediates states with

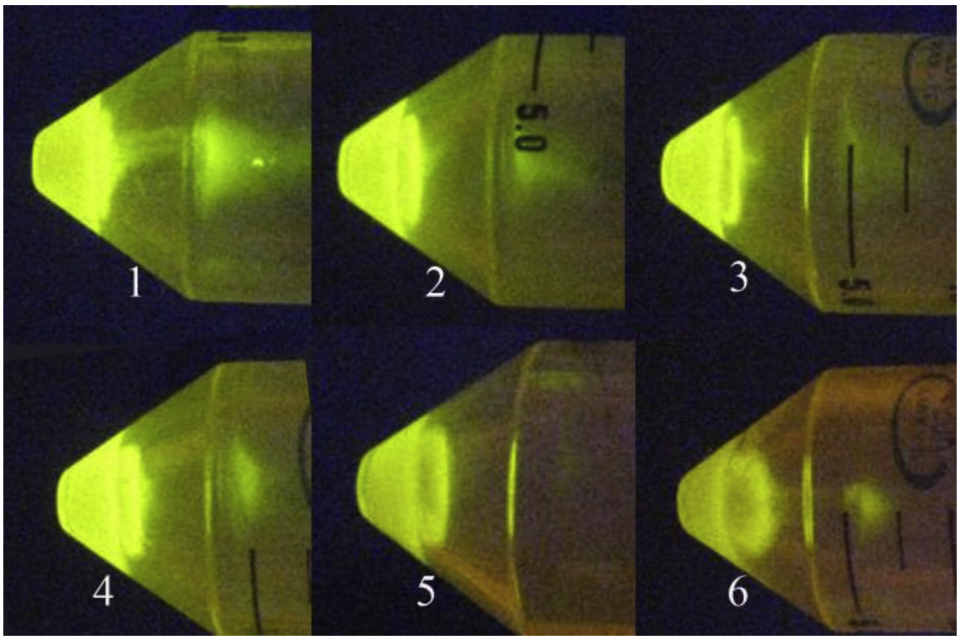

Fig. 2. Fluorescence intensity of Strep-tagged GFP (1), c-235 (2), c-232 (3), c-229 (4), c-227 (5) and c-226 protein (6) after overexpression and centrifugation of the Bl21(DE3) cells. The wet weight was adjusted accordingly. The cells were illuminated with a Dark Reader; without the Dark Reader, the fluorescence of c-226-containing cells would be hard to visualize.

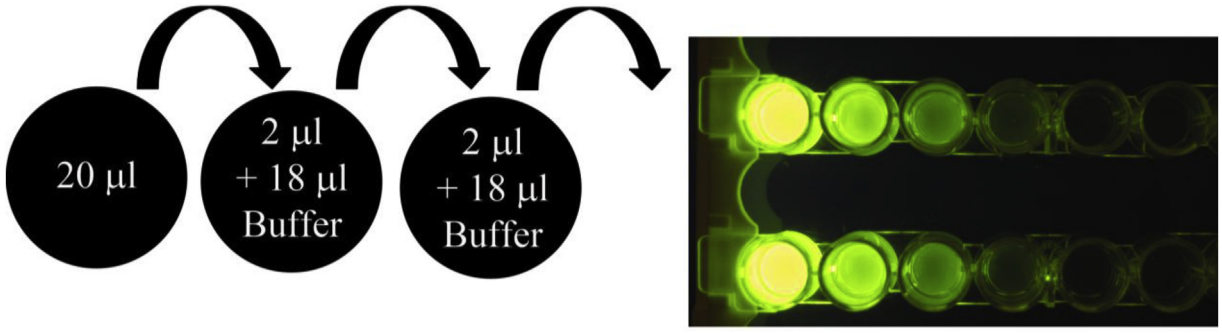

Fig. 3. Serial dilution. We adjusted the concentration of Strep-tagged wild-type GFP and the c-226 mutant to 0.123 mg/ml and performed a serial dilution as described in the figure (upper lane c-226, lower lane GFP wild-type).

increased α-helical secondary content [15,16]; however, the observed decrease in mean residue ellipticity is significant and cannot solely be explained by this mechanism. Similar data can be obtained for the c-226 mutant. The Strep-tag is frequently used for NMR and crystallization and should have no effect on protein structure or activity. Anyhow, as the pET-51b plasmid encodes an enterokinase cleavage side between the Strep-tag and GFP, we cleaved the Strep-tag and re-measured the unfolding curve (Fig. 5A; black curve). Surprisingly, the expected higher mean residue ellipticity for the unfolded state was obtained. The degree of unfolding was calculated for Strep-tagged and Strep-tagged cleaved GFP (Fig. 5B) using Equation (5). At a heating rate of 1 °C/min a change for the half-denaturation temperature $T_{1/2}$ could not be detected (75 °C, pH 6.6). The apparent van't Hoff enthalpy changed dramatically, from 560 kJ/mol for the Strep-tagged GFP to 1258.6 kJ/mol for the untagged GFP (Fig. 5C). Temperature-induced unfolding led to visible aggregates for the GFP, but not for the Strep-tagged GFP. The anomalous thermal aggregation properties of green fluorescent protein are well described in the literature [17]. Nevertheless, both transitions were irreversible. These observations can be explained by a change in the unfolding pathway from $nN \leftrightarrow nD \rightarrow D_n$ for the GFP protein to $N \leftrightarrow D$; $D + D \rightarrow A_2$ and $D + D_j \rightarrow A_n(j = 2,3,4)$ for the Strep-tagged GFP. After unfolding, the Strep-tagged GFP protein rearranged to form a new secondary structure and possible multimers. Finally, we compared the unfolding of the Strep-tagged GFP with the Strep-tagged c-226 mutant at pH 7.6 (Fig. 5D). The apparent van't Hoff enthalpy changed dramatically, from 1151.68 kJ/mol for the Strep-tagged GFP to 600 kJ/mol for the Strep-tagged c-226 (Fig. 5E). The temperature for half-denaturation $T_{1/2}$ changed significantly from 79 °C to 72.8 °C, respectively. The increase in stability for the Strep-

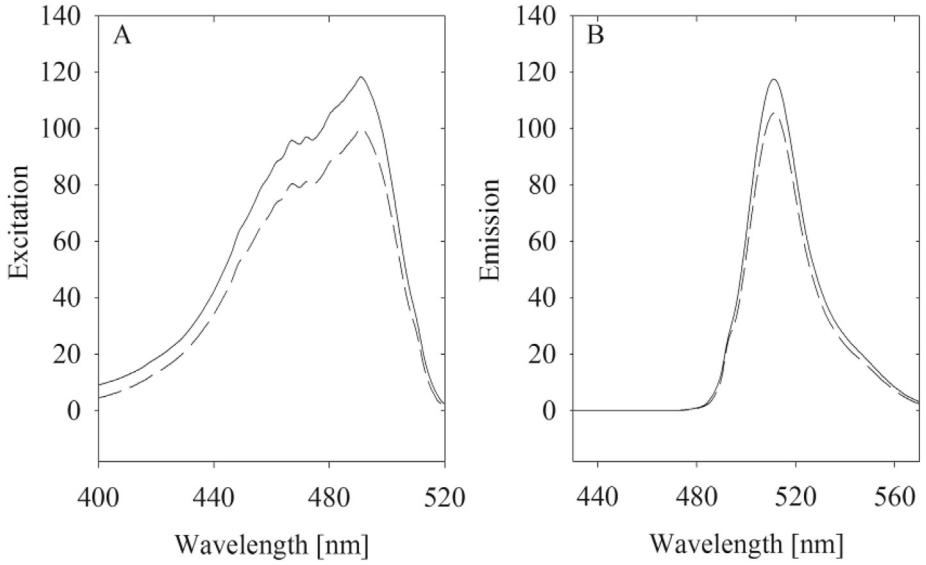

Fig. 4. Excitation (A) and emission (B) spectra of the Strep-tagged wild-type GFP and the c-226 mutant at 0.05 mg/ml. The measurements were performed at 25 °C, with emission and excitation slit widths of 2.5 nm (solid line: wild-type; dashed line: mutant).

tagged GFP as a function of pH – 75 °C at pH 6.6 and 79 °C at pH 7.6 (Fig. 5B, D) – is similar to the literature value for untagged wild-type GFP [18]. Finally, the temperature-jump data (Fig. 5F) displays the huge effect the truncation induces.

As discussed above, for the c-226 mutant, the amount of active folded protein decreased dramatically. To investigate this phenomenon even further, we measured the unfolding kinetics with a jump to 4 M GdnHCl. This ensures fully unfolding without hysteresis [19] but is still slow enough to be mixed by hand. Furthermore, this implies that the unfolding rate constant k_u is much higher than the refolding rate k_f and is well approximated by the observed rate constant k_{obs} [20]. The plot of lnk against 1/T displays strong curvature similar to the refolding for barnase and CI2 [21] (Fig. 6A).

Negative activation enthalpies can be explained due to heat-capacity changes. However, for the Strep-tagged GFP proteins, we noticed that Θ_∞ is a function of the unfolding temperature (Fig. 6C). Our temperature-induced unfolding data revealed that the unfolding of GFP is followed by a rearrangement and possible multimer formation. Thus, an association-limited multimer-formation step, in which association of the unfolded monomers [D] is significantly slower than the conformational changes of the unfolding, can be assumed. GdnHCl-induced unfolding will reduce the likelihood of the $D + D \rightarrow A_2$ and $D + D_j \rightarrow A_n$ transition. At lower temperatures, the enthalpy of transfer of non-polar groups from the protein interior into water is negative and positive above [22], and re-arrangements after unfolding becoming enthalpic unfavorable. It has been observed that a decrease in the temperature reduce the probability for ordered aggregates [23]. This is supported by the constant mean residue ellipticity value Θ_∞ in the lower temperature range (between 5 and 20 degrees). However, at higher temperatures the $D + D \rightarrow A_2$ and $D + D_j \rightarrow A_n$ reaction pathway is possible, as the folding–unfolding equilibrium is shifted. A temperature-induced shift in the reaction pathway explains well the upward concave nonlinear Arrhenius behavior [24]. It has been shown that association-limited kinetics should lead to a non-Arrhenius temperature dependence of k_{obs} due to the temperature dependence of the folding–unfolding equilibrium ($f_{D,eq}$ as a function of temperature, Equation (4)) [13]. Arrhenius energies can be calculated for the lower and higher temperature ranges to compare GFP with the c-226 mutant using the Arrhenius equation (Equation (7)) in the higher and lower temperature ranges as shown in Fig. 6B. We include a typical repetition experiment (triangle and dashed line in Fig. 6B) to support our data. The reproducibility is very good (Fig. 6 and Table 1). Shortening the C-terminal tail decreased the activation energy by 40% in the higher and lower temperature ranges (Table 1).

4. Discussion

The majority of proteins in the PDB database exist in a marginally stable thermodynamic state [25] due to the requirements of enzymes to be flexible and functional [26]. It has been shown that unstructured regions are an important building block for protein stability and function [1], and recent research emphasizes the importance of unstructured regions distal to the active-site [7]. For example, the intrinsically unstructured carboxy-terminus of bacillus lipase is essential for its function [27], the mutations in non-structured regions of troponin T and troponin I are a major cause of familial hypertrophic cardiomyopathy [3], and the C-terminal unstructured region of PTEN plays a major role in for membrane association [28]. Although these proteins are from different protein families, they share a common feature: The tails are not junk, they are an important part of the evolutionary protein design to ensure the right balance between stability and function. A recent review tries to summarize our knowledge

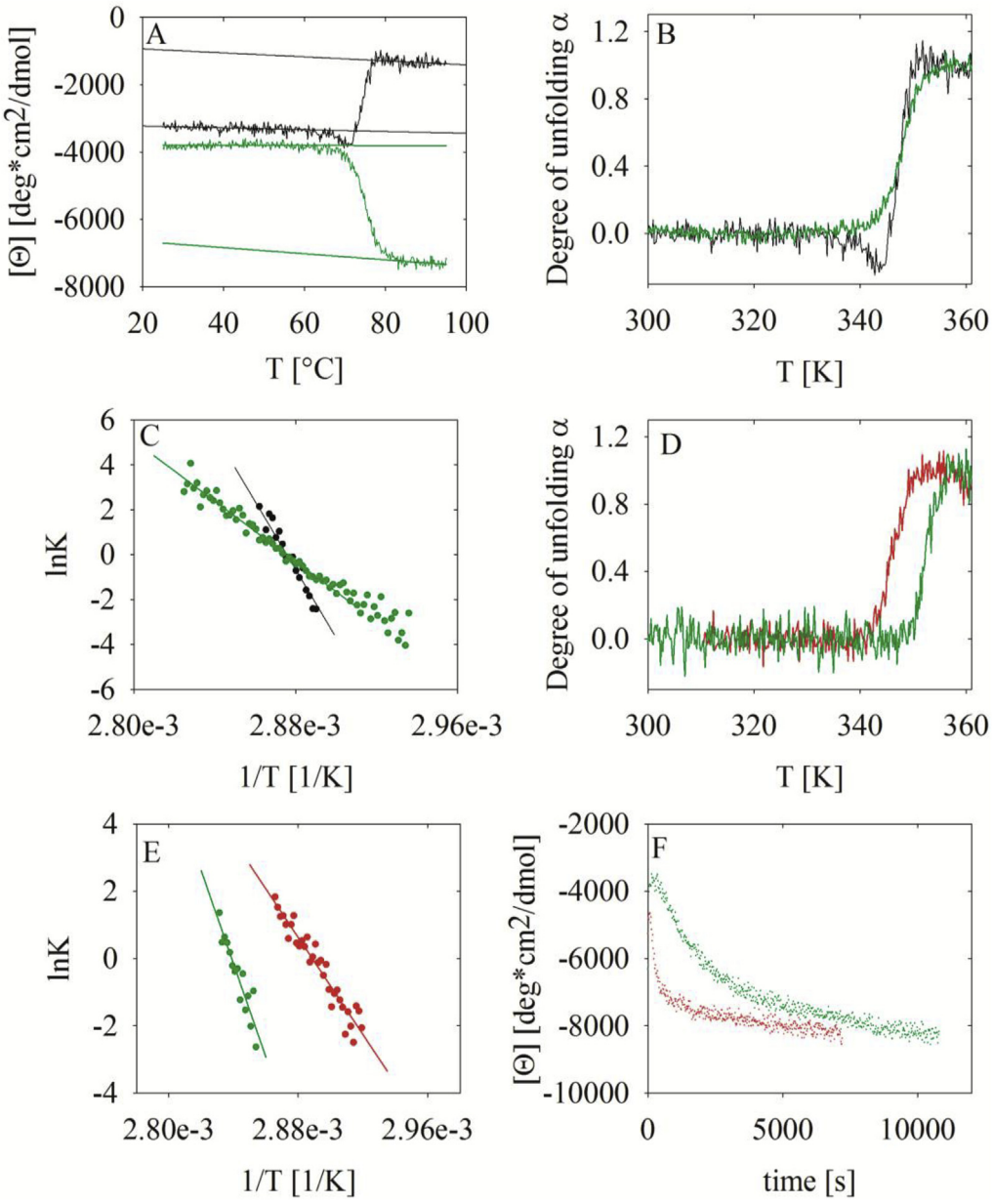

Fig. 5. A. Temperature-induced unfolding of Strep-tagged GFP (green) and GFP (black) as a function of temperature. Linear least square lines are calculated for the unfolded and native state and extrapolated to both ends of the melting curve to calculate the degree of unfolding α. B. The degree of unfolding α as a function of temperature calculated with Equation (5) for the Strep-tagged GFP (green) and GFP (black). C. van't Hoff enthalpy for Strep-tagged GFP (green) and GFP (black) calculated with Equation (6). The temperature-induced unfolding of Strep-tagged GFP (green) and GFP (black) (Fig. 5A, B, C) has been performed in pH 6.6 with a protein concentration of 0.4 mg/ml with a 20 mM MES buffer and 15 mM NaCl. D. Comparison of unfolding curves for the Strep-tagged GFP (green) and Strep-tagged c-226 (red). E. van't Hoff enthalpy for Strep-tagged GFP (green) and Strep-tagged c-226 (red) calculated with Equation (6). F. Temperature jump from 25 °C to 74 °C for the Strep-tagged GFP (green) and Strep-tagged c-226 (red). The Strep-tagged GFP (green) and Strep-tagged c-226 temperature-induced unfolding (Fig. 5D, E, F) have been performed with the standard buffer condition, 10 mM Na_2HPO_4, 10 mM KH_2PO_4, 1 mM EDTA, and 15 mM NaCl, at pH 7.6 and with a protein concentration of 0.3 mg/ml.

about intrinsically disordered protein tails that function as inhibitors/competitors, activators, affinity tuners, signal carriers, DNA wrappers, engagers, and protectors [29].

To our surprise, the eight amino-acid Strep-tag adds an additional step to the unfolding pathway, and a higher-ordered state is formed. If truncation of a flexible tail has a huge impact, an addition of flexible regions could also influence the protein. It has been shown that the His_6-tag can have significant influence in protein constitution [30], and it was concluded that the introduction of the His_6-tag produces, in seldom cases, undesirable changes. Taking our data into account, the effect of affinity tags should be much more carefully investigated, as affinity-tagged proteins are frequently used for x-ray crystallography, NMR, protein−protein interactions (surface plasmon resonance experiments), and high-throughput screening. Hopefully, the extreme effect detected

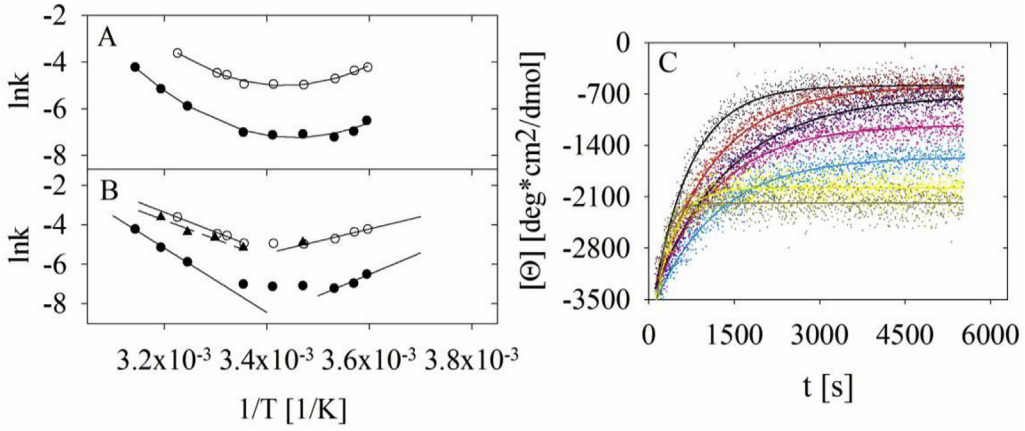

Fig. 6. Unfolding of (Strep-tagged) GFP to 4 M GdnHCl as a function of temperature. The Arrhenius plot for the unfolding (lnk versus 1/T). The black circles show the data for the wild-type, and the open circles and triangle show the data for the mutant. Fig. 6A shows the curvature in the Arrhenius plot, and Fig. 6B shows the activation energy calculated in the higher and lower temperature range. The lines are the best fit to the obtained data. Fig. 6C shows the typical unfolding curves of Strep-tagged GFP as a function of temperature. The lines are the best fit according to Equation (1). Black: 5 °C degree; red: 7 °C degree; blue: 10 °C degree; pink: 20 °C; cyan: 25 °C; yellow: 35 °C; dark yellow: 40 °C.

Table 1
Activation energies calculated by the Arrhenius equation (Equation (7)) in the higher and lower temperature ranges. The value in squared brackets was obtained from the repetition experiment. The value in round brackets is the estimated error for each calculation.

Protein	E_a [kJ/mol] high temperature range	E_a [kJ/mol] low temperature range
Wild-type	135.71 (±13.5)	−90.35 (±9)
c-226	80.19 [83.72] (±8.2)	−51.6 (±5.2)

in this study is a rare case. β-barrels have a complex unfolding and folding pathway. GdnHCl-induced refolding can be extremely complex and involve up to five intermediate states, depending on which GFP has been investigated; affinity-tagged GFP, untagged GFP, or mutations. Unfolding can involve, at low GdnHCl concentrations, up to five intermediate states [31,32]. Furthermore, the backbone required for chromophore synthesis will be exposed during unfolding.

In this paper, we performed measurements of C-terminal deletion mutants of GFP. It has been reported that the fluorescence intensity of C-terminal deletion mutants is strongly reduced. To understand this phenomenon further, we performed a more rigorous quantitative analysis. We have been surprised by the low amount of protein for the truncated mutants (c-226; c-227). Indeed, with identical protein concentration, the observed fluorescence intensity changes are rather small. Comparison with previous literature data is not straightforward, as different GFP proteins have been used – either EGFP [9] or His_6-GFP [14] – and the buffer conditions were different. Certainly, re-evaluation of the previous data is necessary. Proteins with intrinsic fluorescence should be measured with uttermost caution to avoid systematic errors.

Our quantitative analysis by unfolding to 4 M GdnHCl showed that the stability of the protein dramatically changed if the C-terminal tail is truncated. There is the assumption that the lid is involved in some protein–protein interaction [31], and the flexible C-terminus could play an important role. As shown in Fig. 1, the flexible region is located close to the conserved residue Pro-196 (yellow region, Fig. 1) with nearby mutations resulting in ineffective chromophore maturation [31,32]. The flexible region is also close to the backbone (yellow regions, Fig. 1). Therefore, the flexible region could close the barrel and prevent water intrusion. For BamA, a protein in the BAM complex, extracellular loops form a dome over the β-barrel, isolating the interior from the exterior [33]. This should influence the stability and dynamics of the protein. For the GFP cycle3 mutant [17], unfolding involves two intermediate states. In the first stage of unfolding, re-packing of the amino acids leads to swelling, but the secondary structure shows no change. During the following stage, the secondary structure changes, and the protein then unfolds. The first step can especially be influenced by the C-terminal tail, as the interactions described above might tighten the protein. Deleting C-terminal regions induces long-range dynamic effects, which could influence the swelling of the protein in the first step of unfolding [17]. Pressure perturbation studies are important for studying protein folding, stability, aggregation and conformational flexibility. As multidimensional energy-landscapes, folding intermediates, and structural informations of conformers within the native and denatured ensemble can be obtained by high pressure NMR, further high-pressure NMR and structural investigations are useful to understand this dramatic effect [34]. If the unstructured tail prevents water intrusion into the β-barrel interior, differences should be detected, as water intrusion into the cavities is important for the pressure stability.

5. Conclusion

Flexible tails can be important for the function, the stability and/or interaction of a protein. A general theory to predict the role of these dynamic regions is not available, yet. The stability of GFP dramatically changed, if the C-terminal tail was

entirely truncated, but only a small decrease in fluorescence intensity was observed. It might be that flexible, unstructured tails are an important general evolutionary design to adapt the protein to different environmental conditions. Post-translational modifications can remove amino acids from C-terminal tails, whereas changes in the protein interior or in structured regions are difficult and might lead to secondary and tertiary structural changes with unpredictable outcomes.

Author contributions

M.W.L. directed the entire project; M.W.L. and Sh.K. performed the experiments; M.W.L. and Sh.K. analyzed the data; M.W.L. wrote the paper.

Conflict of interest

The authors declare that they have no conflict of interest.

Acknowledgment

This work was supported by the Special Coordination Funds for Promoting Science and Technology from the Ministry of Education, Culture, Sports, Science and Technology of the Japanese government to M.W.L.

References

[1]. K. Gekko, T. Kamiyama, E. Ohmae, K. Katayanagi, Single amino acid substitutions in flexible loops can induce large compressibility changes in dihydrofolate reductase, J. Biochem. 128 (2000) 21−27.
[2]. K.K. Gajewiski, P.J. Saul, Sudden cardiac death in children and adolescents (excluding sudden infant death syndrome), Ann. Pediatr. Cardiol. 3 (2010) 107−112.
[3]. M.W. Lassalle, Defective dynamic properties of human cardiac troponin mutations, Biosci. Biotechnol. Biochem. 74 (2010) 82−91.
[4]. A.V. Gomes, J.D. Potter, Cellular and molecular aspects of familial hypertrophic cardiomyopathy caused by mutations in the troponin I gene, Mol. Cell. Biochem. 263 (2004) 99−114.
[5]. K. El Omari, S. Liekens, L.E. Bird, J. Balzarini, D.K. Stammers, Mutations distal to the substrate site can affect varicella zoster virus thymidine kinase activity; implications for drug design, Mol. Pharmacol. 69 (2006) 1891−1896.
[6]. St.J. Metallo, Intrinsically disordered proteins are potential drug targets, Curr. Opin. Chem. Biol. 14 (2010) 481−488.
[7]. H. van Bedem, G. Bhaba, K. Yang, P.E. Wright, J.S. Fraser, Automated identification of functional dynamic contact networks from x-ray crystallography, Nat. Methods 10 (2013) 896−902.
[8]. G.E. Schulz, β-barrel membrane proteins, Curr. Opin. Struct. Biol. 10 (2000) 443−447.
[9]. X. Li, G. Zhang, N. Ngo, X. Zhao, St.R. Kain, C.C. Hang, Deletions of the aequora victoria green fluorescent protein define the minimal domain required for fluorescence, J. Biol. Chem. 272 (1997) 28545−28549.
[10]. H.-K. Kim, B.-K. Kaang, Truncated green fluorescent protein mutants and their expression in aplysia neurons, Brain Res. Bull. 47 (1998) 35−41.
[11]. R.Y. Tsien, The green fluorescent protein, Annu. Rev. Biochem. 67 (1998) 509−544.
[12]. R. Heim, A.B. Cubitt, R.Y. Tsien, Improved green fluorescence, Nature 373 (1995) 663−664.
[13]. Chr.J. Roberts, in: R.M. Murphy (Ed.), Nonnative Protein Aggregation in Misbehaving Proteins, Springer Science + Business Media, LLC, 2006, pp. 17−47.
[14]. J. Dopf, Th.M. Horiagon, Deletion mapping of aequorea victoria green fluorescent protein, Gene 173 (1996) 39−44.
[15]. J.J. Yang, H. Yang, Y. Ye, H. Hopkins Jr., G. Hastings, Temperature-induced formation of a non-native intermediate state of the all β-sheet protein CD2, Cell Biochem. Biophys. 36 (2002) 1−18.
[16]. L. Zhong, W.C. Johnson Jr., Environment affects amino-acid preference for secondary structure, Proc. Natl. Acad. Sci. U. S. A. 89 (1992) 4462−4465.
[17]. B.S. Melnik, N.V. Molochkov, D.A. Prokhorov, V.N. Uversky, V.P. Kutyshenko, Molecular mechanisms of the anomalous thermal aggregation of green fluorescent protein, Biochem. Biophys. Acta 1814 (2011) 1930−1939.
[18]. K.M. Alkabi, A. Yafea, S.S. Ashraf, Effect of pH on thermal- and chemical-induced denaturation of GFP, Appl. Biochem. Biotechnol. 126 (2005) 149−156.
[19]. S.E. Jackson, T.D. Craggs, J.-R. Huang, Understanding the folding of GFP using biophysical techniques, Expert Rev. Proteomics 3 (2006) 545−559.
[20]. L.A. Wallace, C.R. Matthews, Sequential vs. parallel protein folding mechanisms: experimental tests for complex folding reactions, Biophys. Chem. 101 (2002) 113−131.
[21]. M. Oliveberg, Y.-J. Tan, A.R. Fersht, Negative enthalpies in the kinetics of protein folding, Proc. Natl. Acad. Sci. U. S. A. 92 (1995) 8926−8929.
[22]. G.I. Makhtadze, P.I. Privalov, Contribution of hydration to protein folding thermodynamics I. The enthalpy of hydration, J. Mol. Biol. 232 (1993) 639−657.
[23]. J. Gsnoper, M. Vendruscolo, Theoretical approaches to protein aggregation, Prot. Pept. Lett. 13 (2006) 287−293.
[24]. W. Wang, Chr.J. Roberts, Non-Arrhenius protein aggregation, AAPS J. 15 (2013) 840−851.
[25]. M. de Leeuw, Sh Reuveni, J. Klafter, R. Granke, Coexistence of flexibility and stability of proteins: an equation of states, PLoS One 4 (2009) e7296. http://dx.doi.org/10.1371/journal.pone.0007296.
[26]. A. Ramanathan, P.K. Agarwal, Evolutionary conserved linkage between enzyme fold, flexibility and catalysis, PLoS Biol. 9 (2011) e1001193. http://dx.doi.org/10.1371/journal.pbio.1001193.
[27]. J. Khurana, Manisha, R. Singh, J. Kaur, Intrinsically unstructured carboxy terminus of bacillus lipase is essential for function, Protein Pept. Lett. 21 (2014) 1265−1272.
[28]. P. Malanaey, R.R. Pathak, B. Xue, V.N. Uversky, V. Dave, Intrinsic disorder in PTEN and its interactome confers structural plasticity and functional versatility, Sci. Rep. 3 (2013). http://dx.doi.org/10.1038/srep02035.
[29]. V.N. Uversky, The most important thing is the tail: multitudinous functionalities of intrinsically disordered protein termini, FEBS Lett. 587 (2013) 1891−1901.
[30]. A. Panek, O. Pietrow, P. Filipkowski, J. Synowiecki, Effects of the polyhistidine tag on kinetics and other properties of trehalose synthase from Deinococcus geothermalis, Acta Biochim. Pol. 60 (2013) 163−166.
[31]. O.V. Stepanenko, O.V. Stepanenko, I.M. Kuznetsova, V.V. Verkhusha, K.K. Turoverov, β−barrel scaffold of fluorescent proteins: folding, stability and role in chromophore formation, Int. Rev. Cell Mol. Biol. 302 (2013) 2221−2278.
[32]. Sh-Te.D. Hsu, G. Blaser, S.E. Jackson, The folding, stability and conformational dynamics of β-barrel fluorescent proteins, Chem. Soc. Rev. 38 (2009) 2951−2965.
[33]. N. Noinaj, A.J. Kuszak, J.C. Gumbart, P. Lukacik, H. Chang, N.C. Easley, T. Lithgow, S.K. Buchanan, Structural insight into the biogenesis of β-barrel membrane proteins, Nature 501 (2013) 385−390.
[34]. M.W. Lassalle, K. Akasaka, The use of high-pressure nuclear magnetic resonance to study protein folding, Methods Mol. Biol. 350 (2007) 21−38.